Published online: October 4, 2016

Scientific Report

SOURCE DATA | TRANSPARENT PROCESS

EMBO reports

Cancer-specific mutations in p53 induce the translation of Δ160p53 promoting tumorigenesis

Marco M Candeias[1,2,3,*,†], Masatoshi Hagiwara[2,4] & Michiyuki Matsuda[1,5]

Abstract

Wild-type *p53* functions as a tumour suppressor while mutant *p53* possesses oncogenic potential. Until now it remains unclear how a single mutation can transform *p53* into a functionally distinct gene harbouring a new set of original cellular roles. Here we show that the most common *p53* cancer mutants express a larger number and higher levels of shorter p53 protein isoforms that are translated from the mutated full-length p53 mRNA. Cells expressing mutant p53 exhibit "gain-of-function" cancer phenotypes, such as enhanced cell survival, proliferation, invasion and adhesion, altered mammary tissue architecture and invasive cell structures. Interestingly, Δ160p53-overexpressing cells behave in a similar manner. In contrast, an exogenous or endogenous mutant p53 that fails to express Δ160p53 due to specific mutations or antisense knock-down loses pro-oncogenic potential. Our data support a model in which "gain-of-function" phenotypes induced by p53 mutations depend on the shorter p53 isoforms. As a conserved wild-type isoform, Δ160p53 has evolved during millions of years. We thus provide a rational explanation for the origin of the tumour-promoting functions of p53 mutations.

Keywords Δ160p53; GOFs; mutant p53; p53 isoforms; p53 mRNA
Subject Categories Autophagy & Cell Death; Cancer
DOI 10.15252/embr.201541956 | Received 21 December 2015 | Revised 21 August 2016 | Accepted 6 September 2016

Introduction

When first discovered, *p53* was described as an oncogene because it was overexpressed in cancers and it supported tumorigenic transformation [1,2]. Today, this is still true for a collection of mutant *p53* genes [3], though the wild-type (wt) *p53*, oppositely, has been nominated a tumour suppressor and the guardian of the genome [4]. Indeed, depending on its mutation status, the *p53* gene can act as a tumour suppressor or a pro-oncogene, each role with its distinct and unique features. Maybe because of its two faces, *p53* is the most frequently mutated gene in cancer: a single nucleotide change can metamorphose the hero into a villain [5,6]. To this date, it is not known how such contrasting roles could have evolved in the same gene. Particularly, the oncogenic functions (often referred to as mutant p53 "gain of functions" or GOFs) only seem to manifest themselves after mutation so it is a big mystery how these functions could have been perfected throughout evolution. Considering the amount of oncogenic functions described for mutant p53 so far and all the regulatory mechanisms behind them, one thing appears to be clear though, these "gained" functions are not likely to be the simple direct products of a single chance mutation.

The first p53 protein described, the full-length (FL) p53, turned to be just one of many isoforms encoded by the *p53* gene [7]. More recently, some of the functions of shorter p53 isoforms have been elucidated and they are different from and complement FLp53 activity [8]. Different isoforms are also regulated in different ways, such as alternative splicing or internal ribosome entry site (IRES)-mediated translation [9,10] or transcription from an internal promoter present in intron 4 of *p53* [11]. The internal promoter originates the Δ133p53 mRNA, which codes for proteins Δ133p53 and Δ160p53 and their respective splice variants [12]. Δ133p53 has been attributed to roles in angiogenesis [13] and in the regulation of replicative cellular senescence [14], but very little is known about the later-discovered Δ160p53 even though it is the second most conserved p53 isoform among species, just after FLp53 [12]. Here we show that Δ160p53 controls cell fate in ways very similar to mutant R273Hp53 and provide for the first time a plausible explanation to the long-time dilemma of the origin and evolution of the oncogenic mutant p53 GOFs.

Results and Discussion

Mutant *p53* expresses p53 isoforms via mutated full-length p53 mRNA

It is well established that mutant p53 proteins are expressed at higher levels compared to wild-type (wt) p53 [15,16]. We were interested in investigating whether p53 shorter isoforms are also

1 Laboratory of Bioimaging and Cell Signaling, Graduate School of Biostudies, Kyoto University, Kyoto, Japan
2 Department of Anatomy and Developmental Biology, Graduate School of Medicine, Kyoto University, Kyoto, Japan
3 Departamento de Genética Humana, Instituto Nacional de Saúde Dr. Ricardo Jorge, Lisboa, Portugal
4 Medical Research Support Center, Graduate School of Medicine, Kyoto University, Kyoto, Japan
5 Department of Pathology and Biology of Diseases, Graduate School of Medicine, Kyoto University, Kyoto, Japan
*Corresponding author. Tel: +81 75 753 9298, +351 91 549 5562; E-mail: candeias@gmail.com
†Present address: Molecular and RNA Cancer Unit, Graduate School of Medicine, Kyoto University, Kyoto, Japan

affected by this phenomenon. As expected, lung cancer p53-negative H1299 cells transiently or stably expressing wt p53 or *R273Hp53* cDNAs showed higher steady-state expression levels for the mutant full-length (FL) protein (Fig 1A). But an even more remarkable difference between the two was the appearance of several faster migrating bands in the Western blotting (WB) exclusively on mutant p53-expressing cells. Among those bands, we could confirm the identity of the Δ160p53 isoform (Fig 1A, blue square) by mutating the translation initiation codon for Δ160p53 (M160A) in the mutant background (Fig 1A, lane 3). Two other higher molecular weight bands were affected by the M160A mutation and were also present in lysates from cells transfected with the Δ133p53 or Δ160p53 constructs (Fig 1A, lanes 3–5, marked with *, in blue). Since these plasmid constructs do not express the larger p53

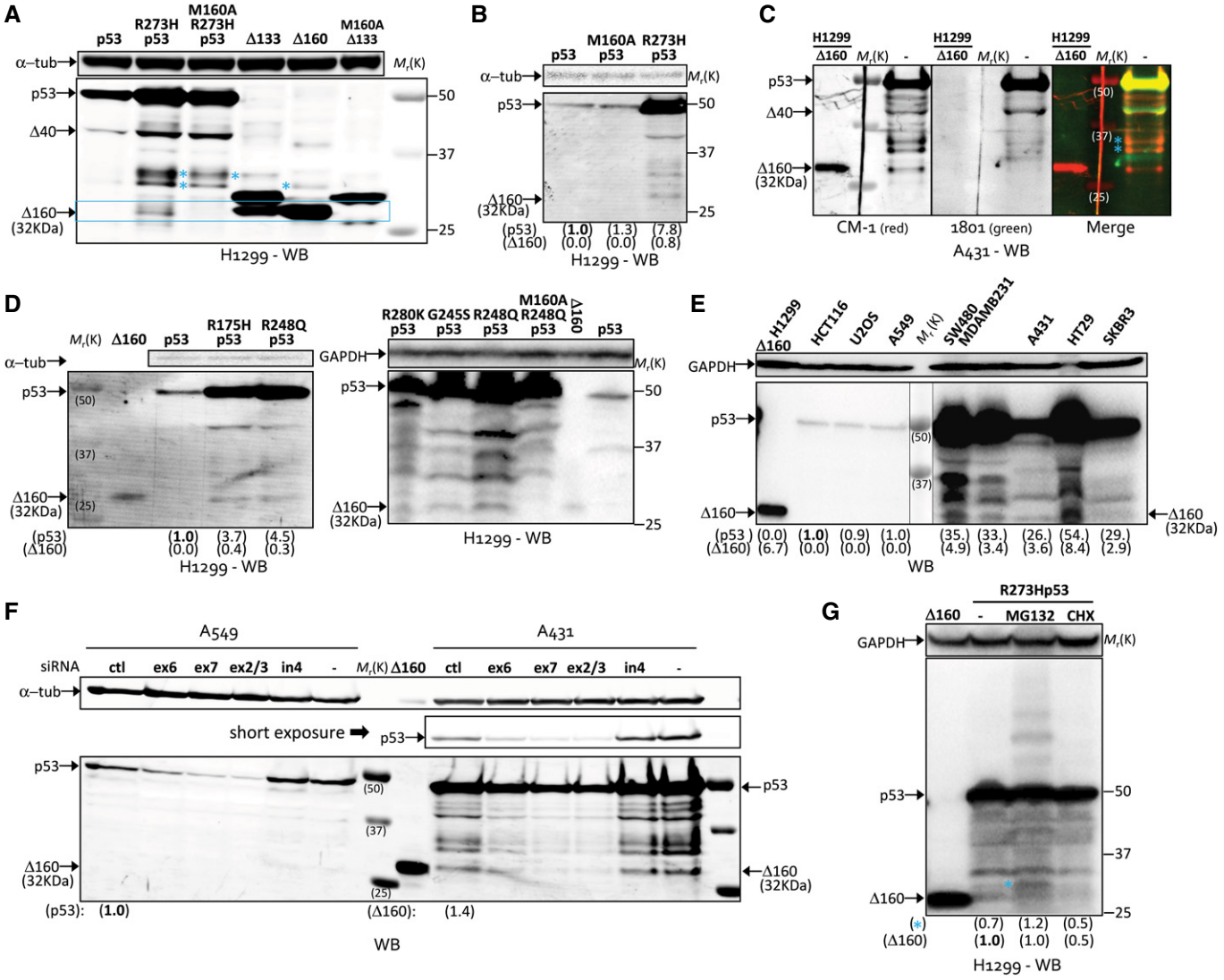

Figure 1. Mutant p53 expresses p53 isoforms.

A, B Western blotting (WB) of p53-negative lung cancer H1299 cells stably expressing (A) or transiently expressing (B) the indicated constructs. Post-translationally modified Δ133p53 and Δ160p53 isoforms are indicated with *.

C The same WB membrane containing lysates from R273Hp53-expressing A431 cells was incubated with rabbit polyclonal CM-1 antibody and mouse monoclonal 1801 antibody against the N-terminus of p53. Detection using anti-rabbit IRDye 680LT (red) and anti-mouse IRDye 800CW (green) secondary antibodies confirmed that the Δ160p53 band corresponds to a C-terminal isoform of p53.

D WB of H1299 cells transiently expressing the indicated constructs.

E WB of cell lines expressing wild-type (HCT116, U2OS, A549) or mutant (SW480 [R273H/P309S], MDAMB231 [R280K], A431 [R273H], HT29 [R273H] and SKBR3 [R175H]) p53.

F Cell lines harbouring endogenous wild-type (A549) or R273H mutant (A431) p53 were treated or not with control siRNA (Ctl) or siRNA targeting both p53 transcripts (ex6 and ex7), full-length mRNA only (ex2/3) or Δ133p53 mRNA only (in4) before lysis and WB.

G WB of H1299 cells stably expressing R273Hp53 and treated with DMSO, proteasome inhibitor MG132 or mRNA translation inhibitor cycloheximide (CHX).

Data information: Shown are representative data of three independent experiments. The numbers in parentheses indicate the amounts of protein for the indicated bands according to WB quantifications and normalization against α-tubulin or GAPDH and relative to the value indicated in bold and set to 1.0. In WBs for endogenous p53 cell lines, the Δ160 lane is used as a marker lane showing Δ160p53 as transiently expressed in p53-null H1299 cells.

isoforms, we can deduce that the two higher molecular weight bands marked with * in lanes 4 and 5 are likely to be post-translational modifications (PTMs) of Δ133p53 and Δ160p53 and contribute to the thicker bands seen in lane 2 when compared to lane 3 (Figs 1A and EV1A). The M160A mutation had no visible effect in wt or mutant FLp53 expression (Fig 1A and B). We reconfirmed the identity of Δ160p53 in a cell line with endogenous R273Hp53 (A431) by using a monoclonal antibody (1801) that binds the N-terminus of p53 and thus can only detect FLp53 and Δ40p53 but not the shorter isoforms: as expected, 1801 failed to detect Δ160p53 (Fig 1C). Interestingly, in this cell line, the weaker band immediately above Δ160p53 was not Δ133p53—as it was labelled by 1801—which means R273H controls Δ160p53 levels by a mechanism that is independent of Δ133p53 expression. The Δ160-related PTMs were only weakly recognized by 1801 antibody, when compared with Δ40p53, for example (Fig 1C, bands marked with *, in blue); this explains the partial, but not total, depletion of these bands in the M160A/R273Hp53 double mutant (Fig 1A, lane 3).

Next we wanted to know whether other missense hotspot cancer mutations in *p53* also induce Δ160p53 expression. We tested the mutations that are most frequent in cancer (R175H, G245S, R248Q, R273H and R280K) and they all showed a strong increase in Δ160p53 levels (Fig 1D). Again, the M160A mutation abrogated Δ160p53 expression in the mutant backgrounds (Fig 1D, right panel, lane 4). Of interest, Δ160p53 levels were half as high, or in some cases almost the same, as wt FLp53 levels (Fig 1B and D), which suggests a potential functionality for this small isoform. This was also observed in five different cell lines endogenously expressing different mutant p53s: SW480 (R273H/P309Sp53), MDAMB231 (R280K), A431 (R273H), HT29 (R273H) and SKBR3 (R175H) (Figs 1E and EV1B). Wt p53 cell lines (HCT116, U2OS and A549) showed no signs of shorter isoform expression. We loaded larger amounts of wt p53 cell lysates but still failed to detect Δ160p53 under regular culture conditions (Fig EV1C).

We further investigated the expression of Δ160p53 in cell lines with endogenous R273H mutant p53. Mutant p53 cell lines A431 and HT29 showed a very similar p53 isoform profile compared to transfected H1299 cells, with clear expression of Δ160p53 (Fig 1F and data not shown). Similar to R273Hp53-transfected H1299 cells where Δ160p53 is expressed from the FL p53 cDNA, Δ160p53 in these cells lines was expressed from the FL p53 mRNA and not the shorter Δ133p53 mRNA originating from the promoter in intron 4, as shown by siRNA experiments targeting both transcripts (ex6 and ex7 siRNAs), FL mRNA only (ex2/3 siRNA) or Δ133p53 mRNA only (in4 siRNA) (Fig 1F). These results are in agreement with the fact that R273H mostly controls Δ160p53 levels and not Δ133p53 (Fig 1C): if R273H were inducing isoform expression via enhanced transcription of the shorter Δ133p53 mRNA, we would expect an increase in both Δ133p53 and Δ160p53, not a specific augmentation of Δ160p53 alone. Having discarded alternative promoter usage as the source for Δ160p53 expression in mutant p53, we then tested the possibilities of enhanced stability or mRNA translation. The proteasome inhibitor MG132 had little or no effect on Δ160p53 levels, but the translation inhibitor cycloheximide (CHX) strongly inhibited the short isoform's expression, showing that it is regulated by translation (Fig 1G). Curiously, MG132 induced the PTM band observed in Fig 1A and C (marked with a blue *). We thought this must be an ubiquitin-modified form since we could also observe ubiquitinated FLp53 bands. We confirmed this by using an inhibitor of the ubiquitin-activating enzyme E1, UBEI-41 (Fig EV1D).

The cell survival capacity of mutant R273Hp53 cells requires Δ160p53 isoform expression

siRNA against p53 induced apoptosis in A431 and HT29 cell lines expressing endogenous R273Hp53 and treated with endoplasmic reticulum (ER) stress inducer drug thapsigargin (Th), confirming the pro-survival quality of mutant p53 (Fig 2A). Next we examined the impact of short p53 isoforms expression in mutant p53 functions. Lung cancer p53-positive A549 cells show a low proliferation rate after reaching cell confluency [17,18], but the same cells stably expressing mutant R273Hp53 continued proliferating exponentially for several days following full confluency, a manifestation of mutant p53 "gain of function" (GOF) (Fig 2B). Interestingly, Δ160p53-expressing cells were also resistant to density-associated diminished proliferation. And surprisingly, mutant p53 lost the GOF when expression of Δ160p53 was revoked by point mutation (M160A/R273Hp53-expressing cells). Similar results were obtained in H1299 cells treated with the tumour promoter and ER stress inducer drug thapsigargin (Fig 2C). Mutant p53- and Δ160p53-expressing cells proliferated more and died less compared to control or M160AR273Hp53 cells. It is important to note that H1299 cells are negative for p53, so the pro-proliferative and/or anti-apoptotic functions of R273Hp53 and Δ160p53 isoform are not dominant negative effects and are not dependent on the interaction/oligomerization with wt FLp53. This also means that these functions are likely independent of the transactivation of p53 target genes since Δ160p53 lacks both p53 transactivation domains [12]. Apoptotic transactivation-independent functions of p53 have been reported previously [19] so we next tested whether Δ160p53 has the capacity to inhibit apoptosis. As expected, wt p53 induced apoptosis in H1299 cells (Fig 2D). In line with the observation that wt p53 expresses extremely low levels of Δ160p53 (Fig 1A and D), deleting Δ160p53 in this context had no effect on apoptosis. Next we tested Δ160p53 expression alone. The inhibition of apoptosis by Δ160p53 in H1299 cells treated with Th was clear (Fig 2E). We were also interested in studying the relative contribution of different isoforms to the observed phenotypes, in particular Δ133p53 that is most similar to Δ160p53 in size and was shown before to be anti-apoptotic [20]. Δ133p53 also reduced apoptosis in our assays, but not to the same extent as Δ160p53 and it lost that capacity once we mutated the initiation codon for Δ160p53, suggesting that the anti-apoptotic capacity of Δ133p53 in H1299 cells is actually mediated by Δ160p53 (Fig 2E).

To further validate the link between mutant and Δ160p53 functions, we sought to test stress conditions when R273Hp53 shows no GOF and verify whether Δ160p53 is still active under those circumstances. The genotoxic drug etoposide (Eto) strongly induced apoptosis in H1299 cells at concentrations of 50 μM but unlike the conditions of over-confluency (Fig 2B) and ER stress (Fig 2C), H273Hp53 showed no effect in this assay (Fig EV2B). Likewise, Δ160p53 was not able to inhibit apoptosis during DNA damage stress, confirming the close link between Δ160p53 expression and mutant p53 functions. The types of stress that activated mutant p53 GOFs in our experiments so far were always sustained for at least 16 h, sometimes several days (Fig 1A–E), whereas the shorter 6-h

Published online: October 4, 2016

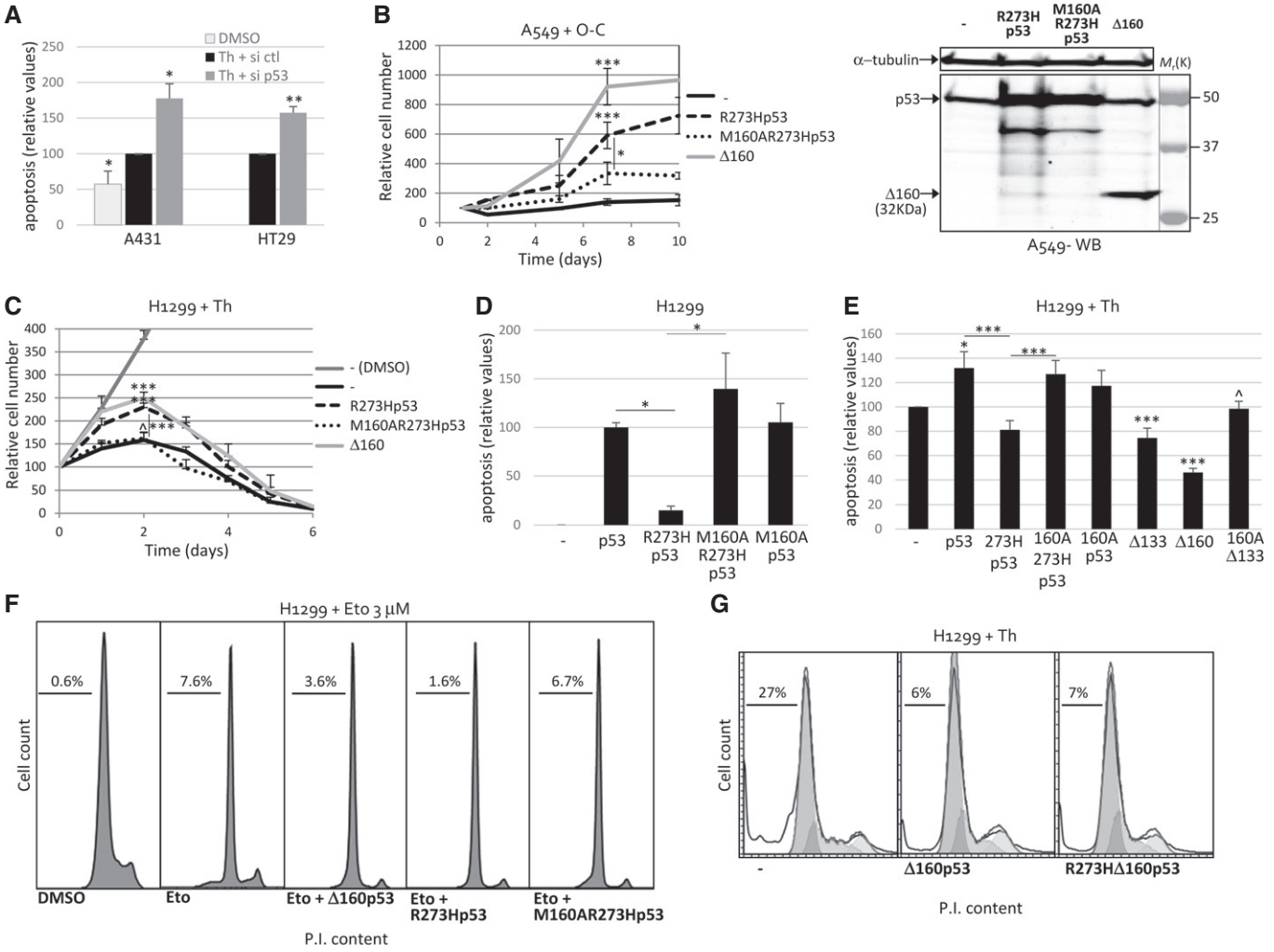

Figure 2. Cell survival capacity of mutant R273Hp53 requires Δ160p53 isoform expression.

A Cell lines endogenously expressing mutant R273Hp53 (A431 and HT29) were treated with control siRNA (Ctl) or siRNA targeting exon 7 of p53, submitted to endoplasmic reticulum (ER) stress by exposure to thapsigargin (Th) and then analysed for apoptosis by incubation with propidium iodide (PI) and FACS analysis. Data were normalized against si Ctl condition, which was set to 100.

B, C A549 (B) and H1299 (C) lung cancer cell lines stably expressing the indicated constructs were counted with trypan blue for several days following stress stimuli (over-confluency (O-C) for A549 and thapsigargin (Th) for H1299). Data were normalized against 1st day values. Δ160p53 shows similar pro-proliferative capacities as mutant R273Hp53. On the other hand, R273Hp53 lost pro-proliferative functions when deficient for Δ160p53 expression (M160AR273Hp53). Also shown is the WB of A549 cells used in (B) and stably expressing the indicated constructs.

D–G H1299 cells transfected with the indicated constructs were submitted to ER stress (E, G), DNA damage by 36 h of 3 μM etoposide (Eto) treatment (F) or cultured under regular conditions (D). Cells were then analysed for apoptosis as in (A). Data were normalized against empty vector (E) or p53 (D) condition, which were set to 100.

Data information: Shown are representative data or averages + s.d. of three independent experiments (*$P < 0.05$, **$P < 0.01$, ***$P < 0.005$ and ^$P > 0.05$ compared to control ("Th + si Ctl" or "−") or as indicated; Student's *t*-test).

treatment with etoposide failed to induce R273Hp53 GOF (Fig EV2B). So we tried a longer etoposide exposure of 36 h at a concentration of 3 μM and retested mutant p53 and Δ160p53's chemoresistance potential. The number of apoptotic cells after treatment was this time smaller (7–8%), and both mutant p53 and Δ160p53 could efficiently inhibit cell death (Fig 2F). Notably, the mutant p53 lacking Δ160p53 (M160A/R273Hp53) failed to protect the cells from the chemotherapeutic agent. As control, we also tested Δ160p53 in the presence of the R273H mutation and saw no difference from wt Δ160p53 (Fig 2G). In all, these data strongly indicate that Δ160p53 contributes to R273H-induced "gain of functions", but not the opposite.

Mutant p53 confers increased adhesion in a Δ160p53-dependent manner in MCF10A cells

While cultivating normal epithelial breast MCF10A cells, we noticed there was a big difference in adhesion between cells stably expressing different p53 cDNAs. We quantified those differences following a previously described protocol [21] and saw that mutant R273Hp53

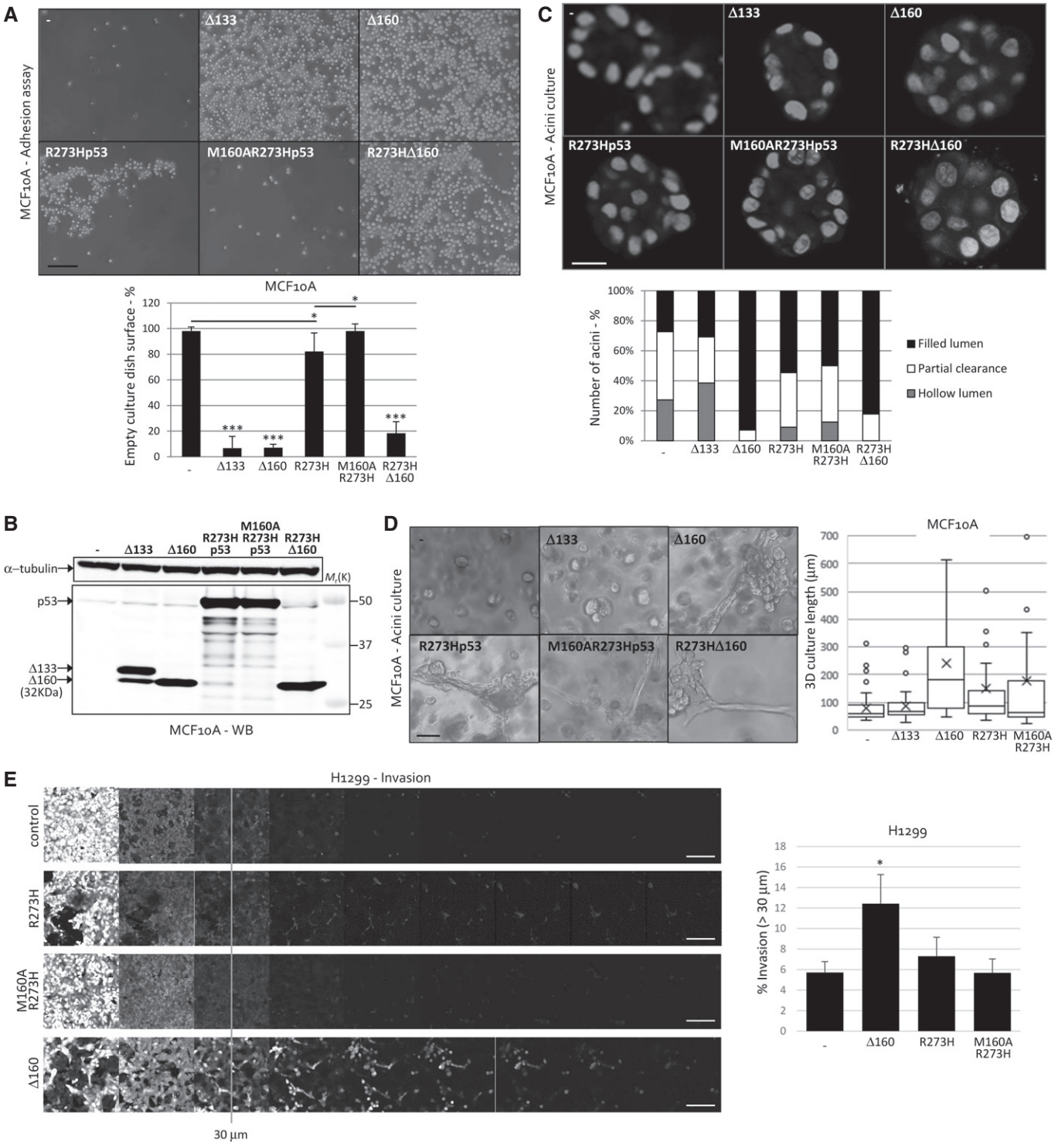

Figure 3.

confers enhanced adhesion to MCF10A cells and isoforms Δ133p53 and Δ160p53 were even more efficient in doing so (Fig 3A and B). Again, mutant p53 without Δ160p53 showed no GOF and R273HΔ160p53 behaved as the wt Δ160p53. In this cell line, minimal levels of Δ160p53 isoform could sometimes be detected in the M160AR273Hp53-expressing cells, and this is likely due to the presence of endogenous Δ133p53 mRNA [20].

Both mutant p53 and Δ160p53 disrupt three-dimensional mammary architecture and induce invasive structures in MCF10A cells

We set to investigate other mutant p53 GOFs. Of particular interest, mutant p53 prevents clearance of cells in the lumen of acini, disturbing the three-dimensional (3D) mammary architecture

Figure 3. Both mutant p53 and Δ160p53 confer increased adhesion and invasion, disrupt three-dimensional mammary architecture and induce invasive structures.

A Adhesion assay shows that MCF10A cells stably expressing Δ133p53, Δ160p53, R273HΔ160p53 or missense mutant R273Hp53 adhere more strongly than control cells. Excluding Δ160p53 expression from the mutant background (M160A/R273Hp53) rescued control cell phenotype. Scale bar represents 200 μm.

B WB of MCF10A cells used in (A) and stably expressing the indicated constructs.

C, D MCF10A human breast epithelial cells stably expressing the indicated constructs were cultured in Matrigel. Control and Δ133p53-expressing cells formed regular three-dimensional (3D) mammary acinar structures with hollow lumina but Δ160p53-, R273HΔ160p53- and to a smaller extent mutant R273Hp53-expressing cells formed acini with filled lumen and long invasive structures ($n > 30$ acini per experiment per condition). Scale bars represent 20 μm (C) and 100 μm (D).

E H1299 cells stably expressing empty vector (control) or the indicated constructs were assessed by confocal micrographs for invasion further than 30 μm through a Matrigel–fibronectin matrix towards EGF-supplemented growth media. The 30-μm plane is indicated and scale bars represent 100 μm. Quantifications are shown in the right panel.

Data information: Shown are representative data and/or averages + s.d. of three independent experiments (*$P < 0.05$ and ***$P < 0.005$ compared to control or as indicated; Student's *t*-test).

[22,23]. Clearance of cells in acini is dependent on apoptosis [24], and since Δ160p53 inhibits apoptosis, we were very curious to test whether here again Δ160p53 contributes to the mutant p53 GOF. Δ160p53's effect on 3D cultures of MCF10A cells was actually much stronger than the disruption caused by mutant p53 (Fig 3C). Indeed, compared to mutant R273Hp53, wt Δ160p53 (or R273HΔ160p53) induced similar but more pronounced phenotypes in different types of assays: increased adhesion (Fig 3A), filled acinar lumina (Fig 3C) and presence of invasive structures [25] (Fig 3D). Disabling Δ160p53 expression in the mutant background could rescue control cell conducts in two-dimensional (2D) cultures (proliferation and adhesion) but had no or minimal effect on mutant 3D traits such as invasive structures and filled acinar lumina. The Δ133p53 cDNA, which expresses Δ160p53 at lower levels (Fig 1A), could mimic Δ160p53 in the adhesion assay but not in the 3D culture assays under the conditions tested.

Ectopic Δ160p53 expression promotes invasion

Another GOF that was reported for mutant p53 is enhanced invasion [25,26]. We tested the capacity of mutant p53 and Δ160p53 to invade through Matrigel–fibronectin matrix towards EGF-supplemented growth media by performing inverted invasion assays. In line with our previous results, Δ160p53-expressing cells manifested the strongest GOF by invading as far as 100 μm in 5 days, while only ~5% of control cells or M160A/R273Hp53-expressing cells migrated past 30 μm (Fig 3E). R273Hp53-expressing cells also showed enhanced invasion (Fig 3E and [25]), though not as impressively as Δ160p53. In sum, mutant p53 and Δ160p53 demonstrated the same six different types of GOFs and also failed to display the same GOF against high-dose chemotherapy (Fig EV2B).

Endogenous R273H-associated pro-oncogenic p53 "gain of functions" require Δ160p53 isoform expression

Finally, to establish a functional interplay between endogenous mutant p53 and endogenous p53 short isoforms, we designed an antisense morpholino oligo (MO) that binds the translation initiation site of Δ160p53 in p53 mRNA and that specifically inhibited the expression of this isoform without affecting Δ133p53 or full-length (FL) p53 levels in H1299 cells or R273Hp53-expressing cell lines A431 and HT29, respectively (Figs 4A and B, and EV3A). The MO was effective and specific in R273Hp53-expressing A431 and HT29 cells but, interestingly, under the conditions tested, it failed to knock down (KD) Δ160p53 in cell lines with different p53 mutations (SW480 [R273H/P309Sp53] and MDAMB231 [R280K]) (Figs 4C and EV3B), implying that sequences in other regions affect the efficiency of the MO. This suggests the presence of ternary RNA structures that

Figure 4. Endogenous R273H-associated pro-oncogenic p53 "gain of functions" require Δ160p53 isoform expression.

A WB of H1299 cells stably expressing Δ133p53 and treated with control morpholino oligos (Ctl-1 or Ctl-2) or antisense morpholino oligo targeting Δ160p53's translation initiation (MO).

B A431 and HT29 cells expressing endogenous mutant R273Hp53 were treated with control morpholinos (Ctl-2 or Ctl-1) or antisense morpholino oligo targeting Δ160p53's translation initiation site (MO) before lysis and WB. Wtp53-expressing A549 cells were used as reference for endogenous wtp53 expression levels. Δ160 lane was used as a marker lane showing Δ160p53 as transiently expressed in p53-null H1299 cells.

C Shown are the average Δ160p53 protein levels expressed in R273Hp53 cell lines that were treated with control morpholino (Ctl-1) or morpholino targeting Δ160p53's translation initiation site (MO). MO efficiently targets Δ160p53 in endogenous R273Hp53 cell lines. See also Fig EV3.

D, E A431 (D) and HT29 (E) cells endogenously expressing mutant R273Hp53 were treated with control siRNA (si Ctl) or control MO (MO Ctl-2 or MO Ctl-1) or siRNA targeting exon 7 of *p53* (si) or MO targeting Δ160p53's translation initiation site (MO), as indicated, submitted to endoplasmic reticulum stress by exposure to thapsigargin (Th) and then analysed for apoptosis by incubation with propidium iodide (PI) and FACS analysis. wtp53-expressing A549 cells were similarly control-treated and used as comparison. Data were normalized against A549 cell condition, which was set to 100.

F A431 and HT29 cells endogenously expressing mutant R273Hp53 were treated with control morpholino Ctl-1 or morpholino targeting Δ160p53's translation initiation site (MO) and then assessed by confocal micrographs for invasion further than 30 μm through a Matrigel–fibronectin matrix towards EGF-supplemented growth media. The 30-μm plane is indicated and scale bars represent 100 μm. Quantifications are shown in the right panel.

G Model illustrating how mutations in p53 induce loss of function but also gain of new functions via isoform expression. The semi-transparent boxes represent plausible minimal full-length p53 and short p53 isoforms activities.

Data information: Shown are representative data or averages + s.d. of three independent experiments (*$P < 0.05$, **$P < 0.01$ and ***$P < 0.005$ compared to A549 (D, E), control (C, F) or as indicated; Student's *t*-test). The numbers in parentheses indicate the amounts of protein for the indicated bands according to WB quantifications and normalization against α-tubulin or GAPDH and relative to the value indicated in bold and set to 1.0.

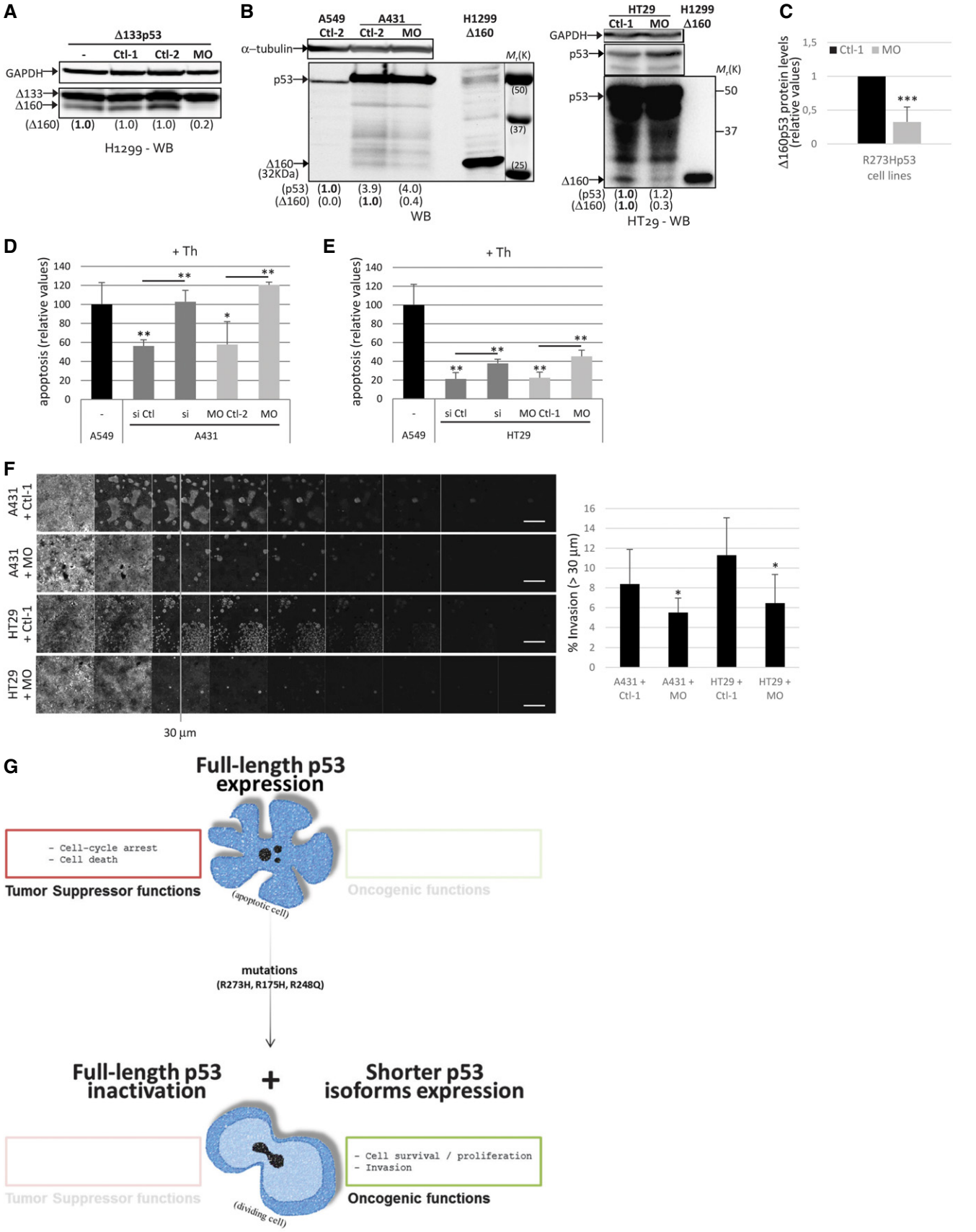
A
Δ133p53
- Ctl-1 Ctl-2 MO
GAPDH
Δ133
Δ160
(Δ160) (1.0) (1.0) (1.0) (0.2)
H1299 - WB
B
A549 A431 H1299
Ctl-2 Ctl-2 MO Δ160
α–tubulin
p53
Δ160 (32KDa)
(p53) (1.0) (3.9) (4.0)
(Δ160) (0.0) (1.0) (0.4)
WB
HT29 H1299
Ctl-1 MO Δ160
GAPDH
p53
p53
Δ160
(p53) (1.0) (1.2)
(Δ160) (1.0) (0.3)
HT29 - WB
C
Δ160p53 protein levels (relative values)
Ctl-1 MO
R273Hp53 cell lines
D
+ Th
apoptosis (relative values)
- si Ctl si MO Ctl-2 MO
A549 A431
E
+ Th
apoptosis (relative values)
- si Ctl si MO Ctl-1 MO
A549 HT29
F
A431 + Ctl-1
A431 + MO
HT29 + Ctl-1
HT29 + MO
30 µm
% Invasion (> 30 µm)
A431 + Ctl-1
A431 + MO
HT29 + Ctl-1
HT29 + MO
G
Full-length p53 expression
- Cell-cycle arrest
- Cell death
Tumor Suppressor functions
(apoptotic cell)
Oncogenic functions
mutations (R273H, R175H, R248Q)
Full-length p53 inactivation
+
Shorter p53 isoforms expression
- Cell survival / proliferation
- Invasion
Tumor Suppressor functions
(dividing cell)
Oncogenic functions

Figure 4.

are affected by the mutations and control protein expression and maybe also access to the MO. Functionally, A431 and HT29 cells (endogenously expressing R273Hp53) were more resistant to thapsigargin (Th) treatment than wtp53 A549 cells, which could be at least partially due to the "gain of function" (GOF) in mutant p53 (Fig 4D and E). Indeed, knock-down of mutant p53 in these cells using siRNA led to an increase in apoptosis. Importantly, specific knock-down of endogenous Δ160p53 using MO was sufficient to inhibit R273H-associated GOF and restore apoptosis, proving that endogenous mutant p53 owes its anti-apoptotic GOF to the Δ160p53 isoform (Fig 4D and E). MO treatment was also equally effective to inhibit the enhanced invasive aptitudes of A431 and HT29 cells (compare H1299 control cells in Fig 3E with Fig 4F).

Altogether, our data indicate that the Δ160p53 isoform, to a greater extent than Δ133p53, can induce mutant-like phenotypes and is possibly the evolutionary origin of at least some of the mutant GOFs since it is a naturally occurring isoform conserved between mammals and that has been subjected to selective pressure for millions of years (Fig 4G).

Conclusions

The data presented here offer a rational explanation to the long-time mystery of how single missense mutations in *p53* can create so many new functions and even new protein interactions (gain of new functions instead of the usual gain of regular function) [27,28]. It is plausible that the "mutant gain of functions" are instead tightly controlled isoform functions that are advantageous to the cell under certain conditions and have evolved within *p53* and are unleashed by the missense mutations, which at the same time also inhibit the more prominent tumour suppressor transcription factor function (Fig 4G). Supporting this proposition, elimination of Δ160p53 expression in a R273H mutant background abrogated p53 "mutant functions" in 2D cultures (Figs 2 and 3A). It is expectable that under different cell stimuli, other isoforms, and not just Δ160p53, contribute to the "mutant functions". For example, even though Δ160p53 could mimic and amplify "mutant functions" in 3D mammary cultures, removing its expression was in this case not enough to completely nullify the mutant phenotype (Fig 3C and D). Interestingly, other frequently occurring p53 mutants, R175Hp53 and R248Qp53, also showed higher levels of Δ160p53 expression, suggesting that this isoform is widely involved in mutant GOFs (Figs 1D and EV1B).

Our study carries significant implications for cancer therapy [29] as we show that a wild-type (Δ160p53) and not mutant p53 protein bears pro-oncogenic traits. From now, efforts can be turned into counteracting isoforms' functions.

Materials and Methods

Cellular assays and reagents

All cell lines were acquired from the American Type Culture Collection (ATCC). All the cell lines with the exceptions of MCF10A were maintained at 37°C and 5% CO_2 in Dulbecco's modified Eagle's media (DMEM) with 10% foetal bovine serum, 5 mM L-glutamine and Pen/Strep 100× solution diluted 1:100. MCF10A cells were cultured in MDEM/F12 supplemented with 5% horse serum, 20 ng/ml EGF, 0.5 μg/ml hydrocortisone, 100 ng/ml cholera toxin, 10 μg/ml insulin and Pen/Strep 100× solution diluted 1:100. Thapsigargin (Sigma; 0.5–1 μM) in A431 and HT29 cells was administered for 20 h and in H1299 cells for 16 h to 6 days, depending on the assay. Over-confluency (O-C) was obtained by keeping the cells in culture for at least 2 days after reaching 100% confluency (with constant media changes). Transient transfections were performed using 293fectin (Invitrogen) according to the manufacturer's protocol. To establish stable polyclonal cell lines, pcDNA3.1 plasmids cloned with the desired inserts were linearized with PvuI (New England Biolabs) before transfection with 293fectin (Invitrogen) (or Lipofectamine 3000 (Life Technologies) if MCF10A cells), and two days later, cells were selected using neomycin (G418; Sigma; 1 mg/ml (0.4 mg/ml for MCF10A)). Control non-transfected cells died after treatment and established cells showed similar levels of transgene expression as confirmed by Western blotting (WB). Once every two months, DNA was extracted from H1299 cells stably expressing wt p53 by using the DNeasy Blood & Tissue Kit (Qiagen) and subjected to PCR and sequencing to confirm that no mutation occurred during selection and maintenance. For WB, cells were lysed in 1.5× SDS sample buffer (62.5 mM Tris–HCl (pH 6.8), 12% glycerol, 2% SDS, 0.004% bromophenol blue and 10% 2-mercaptoethanol) or in buffer A (1% Nonidet P-40, 150 mM NaCl, 20 mM Tris pH 7.4 in the presence of Complete protease inhibitor cocktail (Roche, Mannheim, Germany) followed by Bradford protein assay. After sonication, proteins were separated by SDS–PAGE on 12.5% Nagaiki precast gels (Oriental Instruments Ltd.) and transferred to PVDF membranes (Immobilon-FL, Millipore). After blocking with Odyssey blocking buffer (LI-COR) for 1 h, membranes were blotted with antibodies diluted in a solution of Odyssey blocking buffer and Tris-buffered saline, followed by incubation with secondary antibodies. Membranes were then scanned with an Odyssey IR scanner and analysed with Odyssey imaging software. Primary antibodies (and dilutions) used were rabbit CM-1 [30] for all p53 isoforms (1:8,000), mouse 1801 for N-terminal p53 isoforms (1:500) and mouse anti-α-tubulin (Calbiochem DM1A; 1:2,000). Secondary antibodies used were IRDye 800CW and IRDye 680 (LI-COR). All p53 constructs are cDNAs and were cloned into pcDNA3.1. Morpholino antisense oligo was designed to target Δ160p53 translation initiation site and block translation initiation (MO; Gene Tools, OR, USA, 5′-TGTGGAATCAACCCACAGCTG CACA-3′). Negative control morpholino oligos used consist of a mutated version of the MO against Δ160p53 (Ctl-1; Gene Tools, OR, USA, 5′-TGAGGTATCAACGCACAGCAGCTCA-3′) or target a human beta-globin intron mutation that causes beta-thalassaemia (Ctl-2; Gene Tools, OR, USA; 5′-CCTCTTACCTCAGTTACAAT TTATA-3′). Five microlitres (both 5 and 2.5 μl for Fig EV3) of MO was added to the cells in 1 ml culturing media followed by 5 μl Endo-Porter delivery reagent, and cells were harvested 3 days after. siRNA (GeneDesign or Ambion) was delivered using Lipofectamine RNAiMAX (Life Technologies) following the manufacturer's protocol. siRNA sequences for control and human p53 are as follows:

Control (Ctl): 5′-CACCUAAUCCGUGGUUCAA-3′
p53 (ex6, s606 from Ambion): 5′-GAAATTTGCGTGTGGAGTA-3′
p53 (ex7): 5′-GCATGAACCGGAGGCCCAT-3′

p53 (ex2/3): 5′-GGAAACTACTTCCTGAAAA-3′
p53 (in4): 5′-TGTTCACTTGTGCCCTGACTTTCAA-3′

Adhesion assay

Adhesion assay (resistance to trypsin treatment) was performed as previously published [21]. Briefly, confluent MCF10A cells plated on 6-cm dishes were washed with PBS and incubated with 1 ml trypsin (0.05%, w/v; 0.53 mM EDTA) for 30 min at 37°C. Cells were then washed again two times with PBS and photographs were taken. Quantifications were performed with Adobe Photoshop CS5 software.

Three-dimensional culture

The three-dimensional (3D) culture protocol was carried out as previously described with some modifications [31]. Briefly, MCF10A cells were seeded at a density of 10,000 cells/well in 8-well chamber slides together with 20 µl growth factor-reduced Matrigel (BD Biosciences). Following 20-min incubation at 37°C, growth media were added and cells were allowed to form 3D structures for 5–12 days with constant media changes every 2–3 days. Cells were then fixed with cold 70% ethanol for 15 min at 4°C and stained with propidium iodide (PI; Sigma-Aldrich; 50 mg/ml) for 15 min at room temperature before visualization with an Olympus IX81 confocal inverted microscope equipped with an FV1000.

Cell cycle, cell proliferation and cell death analyses

Cells were harvested and fixed with ice-cold 70% ethanol. After 30-min incubation with RNase at 37°C, cells were stained with propidium iodide (PI, Sigma-Aldrich; 50 mg/ml) and cell cycle distribution was analysed using FACSAria II flow cytometer (BD Biosciences) and FlowJo Software [32]. The sub-G0/G1 population represents cells undergoing apoptosis. Cell proliferation was followed by counting trypsinized cells using trypan blue and Countess Automated Cell Counter (Invitrogen) at different dilutions and in triplicate.

Inverted invasion assays

Matrigel assays were performed as described previously [33]. Briefly, cells were treated and seeded on the base of Matrigel plus fibronectin-filled transwell chambers and invasion towards a gradient of 10% FCS and 25 ng/ml EGF was measured after 5 days by confocal microscopy in serial sections.

Expanded View for this article is available online.

Acknowledgements
This research was supported mainly by Grant-in-Aid for Scientific Research on the Innovative Area of "Resonance Biology" (No. 15H0594) of the Ministry of Education, Culture, Sports, Science and Technology (MEXT) attributed to M.M.; but also by JSPS KAKENHI Grant-in-Aid for Scientific Research (S) Grant Number 15H05721 attributed to M.H. and Grant PTDC/BIM-ONC/4890/2014 from the Fundação para a Ciência e a Tecnologia (FCT) attributed to M.M.C. M.M.C. was supported by grants from the Japan Society for the Promotion of Science (JSPS Postdoctoral Fellowship), AXA Research Fund and the Ichiro Kanehara Foundation.

Author contributions
MMC designed and performed the research. All the authors (MMC, MH, MM) discussed results and commented on the manuscript. MMC wrote the manuscript.

Conflict of interest
The authors declare that they have no conflict of interest.

References

1. Levine AJ, Oren M (2009) The first 30 years of p53: growing ever more complex. *Nat Rev Cancer* 9: 749 – 758
2. Hainaut P, Wiman KG (2009) 30 years and a long way into p53 research. *Lancet Oncol* 10: 913 – 919
3. Muller PA, Vousden KH (2014) Mutant p53 in cancer: new functions and therapeutic opportunities. *Cancer Cell* 25: 304 – 317
4. Lane D, Levine A (2010) p53 Research: the past thirty years and the next thirty years. *Cold Spring Harb Perspect Biol* 2: a000893
5. Weissmueller S, Manchado E, Saborowski M, Morris JPT, Wagenblast E, Davis CA, Moon SH, Pfister NT, Tschaharganeh DF, Kitzing T *et al* (2014) Mutant p53 drives pancreatic cancer metastasis through cell-autonomous PDGF receptor beta signaling. *Cell* 157: 382 – 394
6. Lee MK, Teoh WW, Phang BH, Tong WM, Wang ZQ, Sabapathy K (2012) Cell-type, dose, and mutation-type specificity dictate mutant p53 functions in vivo. *Cancer Cell* 22: 751 – 764
7. Arai N, Nomura D, Yokota K, Wolf D, Brill E, Shohat O, Rotter V (1986) Immunologically distinct p53 molecules generated by alternative splicing. *Mol Cell Biol* 6: 3232 – 3239
8. Marcel V, Dichtel-Danjoy ML, Sagne C, Hafsi H, Ma D, Ortiz-Cuaran S, Olivier M, Hall J, Mollereau B, Hainaut P *et al* (2011) Biological functions of p53 isoforms through evolution: lessons from animal and cellular models. *Cell Death Differ* 18: 1815 – 1824
9. Candeias MM (2011) The can and can't dos of p53 RNA. *Biochimie* 93: 1962 – 1965
10. Sharathchandra A, Katoch A, Das S (2014) IRES mediated translational regulation of p53 isoforms. *Wiley Interdiscip Rev RNA* 5: 131 – 139
11. Bourdon JC, Fernandes K, Murray-Zmijewski F, Liu G, Diot A, Xirodimas DP, Saville MK, Lane DP (2005) p53 isoforms can regulate p53 transcriptional activity. *Genes Dev* 19: 2122 – 2137
12. Marcel V, Perrier S, Aoubala M, Ageorges S, Groves MJ, Diot A, Fernandes K, Tauro S, Bourdon JC (2010) Delta160p53 is a novel N-terminal p53 isoform encoded by Delta133p53 transcript. *FEBS Lett* 584: 4463 – 4468
13. Bernard H, Garmy-Susini B, Ainaoui N, Van Den Berghe L, Peurichard A, Javerzat S, Bikfalvi A, Lane DP, Bourdon JC, Prats AC (2013) The p53 isoform, Delta133p53alpha, stimulates angiogenesis and tumour progression. *Oncogene* 32: 2150 – 2160
14. Fujita K, Mondal AM, Horikawa I, Nguyen GH, Kumamoto K, Sohn JJ, Bowman ED, Mathe EA, Schetter AJ, Pine SR *et al* (2009) p53 isoforms Delta133p53 and p53beta are endogenous regulators of replicative cellular senescence. *Nat Cell Biol* 11: 1135 – 1142
15. Frum RA, Grossman SR (2014) Mechanisms of mutant p53 stabilization in cancer. *Sub-Cell Biochem* 85: 187 – 197
16. Wiech M, Olszewski MB, Tracz-Gaszewska Z, Wawrzynow B, Zylicz M, Zylicz A (2012) Molecular mechanism of mutant p53 stabilization: the role of HSP70 and MDM2. *PLoS One* 7: e51426
17. Camacho-Concha N, Olivos-Ortiz A, Nunez-Rivera A, Pedroza-Saavedra A, Gutierrez-Xicotencatl L, Rosenstein Y, Pedraza-Alva G (2013) CD43

promotes cells transformation by preventing merlin-mediated contact inhibition of growth. *PLoS One* 8: e80806

18. Richter AM, Walesch SK, Wurl P, Taubert H, Dammann RH (2012) The tumor suppressor RASSF10 is upregulated upon contact inhibition and frequently epigenetically silenced in cancer. *Oncogenesis* 1: e18
19. Green DR, Kroemer G (2009) Cytoplasmic functions of the tumour suppressor p53. *Nature* 458: 1127 – 1130
20. Aoubala M, Murray-Zmijewski F, Khoury MP, Fernandes K, Perrier S, Bernard H, Prats AC, Lane DP, Bourdon JC (2011) p53 directly transactivates Delta133p53alpha, regulating cell fate outcome in response to DNA damage. *Cell Death Differ* 18: 248 – 258
21. Sava G, Frausin F, Cocchietto M, Vita F, Podda E, Spessotto P, Furlani A, Scarcia V, Zabucchi G (2004) Actin-dependent tumour cell adhesion after short-term exposure to the antimetastasis ruthenium complex NAMI-A. *Eur J Cancer* 40: 1383 – 1396
22. Zhang Y, Yan W, Chen X (2011) Mutant p53 disrupts MCF-10A cell polarity in three-dimensional culture via epithelial-to-mesenchymal transitions. *J Biol Chem* 286: 16218 – 16228
23. Freed-Pastor WA, Mizuno H, Zhao X, Langerod A, Moon SH, Rodriguez-Barrueco R, Barsotti A, Chicas A, Li W, Polotskaia A *et al* (2012) Mutant p53 disrupts mammary tissue architecture via the mevalonate pathway. *Cell* 148: 244 – 258
24. Debnath J, Mills KR, Collins NL, Reginato MJ, Muthuswamy SK, Brugge JS (2002) The role of apoptosis in creating and maintaining luminal space within normal and oncogene-expressing mammary acini. *Cell* 111: 29 – 40
25. Muller PA, Caswell PT, Doyle B, Iwanicki MP, Tan EH, Karim S, Lukashchuk N, Gillespie DA, Ludwig RL, Gosselin P *et al* (2009) Mutant p53 drives invasion by promoting integrin recycling. *Cell* 139: 1327 – 1341
26. Coffill CR, Muller PA, Oh HK, Neo SP, Hogue KA, Cheok CF, Vousden KH, Lane DP, Blackstock WP, Gunaratne J (2012) Mutant p53 interactome identifies nardilysin as a p53R273H-specific binding partner that promotes invasion. *EMBO Rep* 13: 638 – 644
27. Muller PA, Vousden KH (2013) p53 mutations in cancer. *Nat Cell Biol* 15: 2 – 8
28. Brosh R, Rotter V (2009) When mutants gain new powers: news from the mutant p53 field. *Nat Rev Cancer* 9: 701 – 713
29. Khoo KH, Verma CS, Lane DP (2014) Drugging the p53 pathway: understanding the route to clinical efficacy. *Nat Rev Drug Discov* 13: 217 – 236
30. Midgley CA, Fisher CJ, Bartek J, Vojtesek B, Lane D, Barnes DM (1992) Analysis of p53 expression in human tumours: an antibody raised against human p53 expressed in *Escherichia coli*. *J Cell Sci* 101: 183 – 189
31. Debnath J, Muthuswamy SK, Brugge JS (2003) Morphogenesis and oncogenesis of MCF-10A mammary epithelial acini grown in three-dimensional basement membrane cultures. *Methods* 30: 256 – 268
32. Nicoletti I, Migliorati G, Pagliacci MC, Grignani F, Riccardi C (1991) A rapid and simple method for measuring thymocyte apoptosis by propidium iodide staining and flow cytometry. *J Immunol Methods* 139: 271 – 279
33. Caswell P, Norman J (2008) Endocytic transport of integrins during cell migration and invasion. *Trends Cell Biol* 18: 257 – 263

